Proceedings of the
47th IEEE Conference on Decision and Control
Cancun, Mexico, Dec. 9-11, 2008



# A Fast Method for the Solution of some Tomography Problems

Didier Georges

*Abstract*— **Tomography is an imaging technique, commonly used in medical applications, but also in geophysics and astrophysics. This technique allows estimation of internal characteristics of an object apart from measurements performed outside the object. Its main interest lies in the fact that the estimation process does not require any intrusive operations. From a methodological point of view, tomography may be divided into two main stages: first a forward model has to be provided (i.e. a model of the observed physical phenomena generally based on one or several partial differential equations); then an inverse model based on the forward model is derived which consists in reconstructing physical characteristics of the object. In general such an inverse model is a large-scale ill-posed problem. This paper is devoted to a new approach based on the derivation of a low complexity forward model. The inverse problem is then solved very efficiently with reduced computation time compared to classical approaches based on the finite element method (FEM). The here-proposed approach is applicable to problems governed by elliptic partial differential equations. An example of 2D bioluminescence tomography illustrates the effectiveness of the approach.**

*Index Terms*— **Tomography, elliptic partial differential equations, model reduction, inverse problems, parameter estimation, identification.**

## I. INTRODUCTION

Applications of tomography are various. Optical tomography [1] is used for non-intrusive tumor detection in tissues. In geophysical prospecting successful applications are reported for non-intrusive rock elasticity analysis [12]. In astrophysics, Zeeman-Doppler imaging technique is used for magnetic field estimation on star surface [4].

This paper is devoted to a low complexity approach allowing a good location of physical parameters inside an object, with reduced computation time. The forward model is solved by using a spectral Galerkin method, where we seek for an approximate solution in an orthonormal basis. Then, the parameters to be reconstructed are a linear combination of the same basis functions. As a consequence of the use of an orthonormal basis of approximation functions, the complexity of both the forward and inverse problem are reduced to a minimum.

In most of the existing approaches, computation of the forward model is performed by using either the finite-difference method (FDM) or the finite-element method (FEM, [2]). These two methods are based on a discretization of the domain. A regular grid is used in the FDM, where a complex irregular mesh made of triangles is used in the FEM. For both methods, quality of the solution strongly depends on grid or mesh density. As a consequence *the complexity of the inverse problem is governed by the number of nodes*.

Computation of the inverse problem reduces in most of the cases to solving a large-scale linear least-square problem, corresponding to a so-called perturbation equation of the form:

$$Wx = y_m, \tag{1}$$

where $x$ denotes the $L \times 1$ vector of differences between the physical parameters of a reference medium and those of the imaged medium, $y_m$ is the $m \times 1$ vector of the measured signals and $W$ is the $L \times m$ sensitivity matrix of measurements with respect to unknown parameters. In general, the perturbation equation is both under determined and ill-posed [13]. The so-called ART approach (Algebraic Reconstruction Technique) is often used to compute inverse problems. This approach is based on sensitivity analysis which lead to the computation of some adjoint partial differential equations [10]. Many other iterative methods have been introduced, such as the conjugated-gradient method [14] or the regularized least-square method [15].

In this paper, we focus our attention on the reduction of the forward model, as a way to reduce the overall complexity of the inverse problem. A similar idea has been followed in [6], [7], where a multi-resolution approach based on wavelets has been proposed for the reduction of the FEM rigidity matrix. However in the here-proposed approach, *computation of the forward model does not require any grid*.

In what follows, attention is focused to tomography applications governed by elliptic partial differential equations, such as equations governing light propagation in scattering medium in optical tomography.

### A. Bioluminescence Tomography

Bioluminescence imaging is based on the detection of the light emitted during catalyze of luciferine by the enzyme luciferase [3].

This work was supported by CEA-LETI, Grenoble, France

D. Georges is with Grenoble Institute of Technology, CNRS, GIPSA-lab, Control Systems Dept, BP 46, 38402 Saint Martin d'Heres, France didier.georges@inpg.fr

This method gives the opportunity to measure efficiency of a genic therapy or to observe the growth or migration of cancer cells expressing luciferase.

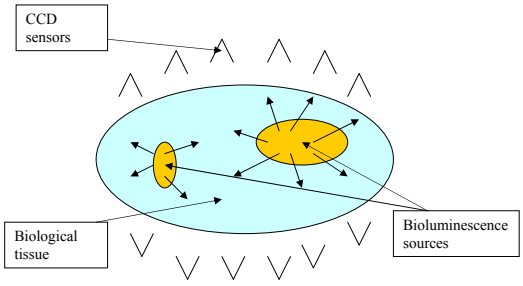


Fig. 1. Bioluminescence tomography principle

The problem consists in reconstructing light sources in a domain $\Omega$ apart from measurements of the scattered light coming from the sources on the periphery of the domain. Light propagation through a scattering medium is governed by an elliptic partial differential equation arising from an approximation of the so-called radiative transport equation:

$$-\nabla.(D(r)\nabla u(r)) + k(r)u(r) = q(r), \tag{2}$$

where $u(r)$ is the fluence rate, $D(r)$ and $k(r)$ are the diffusion and absorption coefficients. $q(r)$ denotes the light intensity of sources. Boundary conditions of Robin-type are taken into account:

$$u(r) + 2D(r)n.\nabla u(r) = 0,\ \forall r \in \partial\Omega, \tag{3}$$

where $n$ is the vector orthogonal to the domain boundary and pointing outward. In order to simplify the computation of the forward model, a common treatment consists in interpreting the Robin boundary conditions as Dirichlet boundary conditions on extrapolated domain. : $u(r) = 0, \forall r \in \partial\Omega$. An output equation is also introduced:

$$y = Cu(r),\ \forall r \in \partial\Omega, \tag{4}$$

where $C = (\delta(r - r_1), ..., \delta(r - r_m))^T$ denotes the operator defined by locations $r_i$, $i = 1, ..., m$ of $m$ CCD sensors located on the periphery of the domain and $y$, the measured fluence rates. $\delta(.)$ is Dirac's operator.

The inverse problem consists in solving the following parametric optimization problem in the least-square sense:

$$\min_{q \in L^2(\Omega)} \|y_m - Cu_m(r, q)\|^2, \tag{5}$$

where $y_m$ is the vector of measurements performed by the CCD sensors.

Now we consider the general class of inverse problem defined by:

$$\min_{q \in L^2(\Omega)} \|y_m - y(r, q)\|^2, \tag{6}$$

where $u(r, q)$ is solution of an elliptic PDE of the form (2):

$$-\nabla.(D\nabla u(r)) + ku(r) = Bq(r),\ \forall r \in \Omega \tag{7}$$

$$u(r) = 0,\ \forall r \in \partial\Omega, \tag{8}$$

$$y = Cu(r). \tag{9}$$

Furthermore the coefficients $D$ and $k$ are supposed to be known and constant over the domain.

## II. A LOW COMPLEXITY SPECTRAL GALERKIN METHOD

Here we consider the use of a Galerkin method [11] defined on *a basis of orthonormal functions, without any explicit grid of the domain*.

The Galerkin method seeks for an approximate solution $u_a$ of problem defined by (7)-(9) as a linear combination of basis functions $\phi_i(r)$ :

$$u_a(r) = \sum_{i=1}^{N} u_i \phi_i(r), \tag{10}$$

where $U = (u_1, ..., u_N)^T$ denotes the vector of the unknown coordinates of the solution in the basis.

Introducing the approximate solution $u_a$ in equation (7) leads to a residual $R(U, r) = -\nabla.(D\nabla u_a(r)) + ku_a(r) - Bq(r)$ that should be reduced to a minimum.

A way to get a minimal residual is to render it orthogonal to each basis function:

$$\int_\Omega R(U, r)\phi_i(r)d\Omega = 0,\ \forall i = 1, ..., N. \tag{11}$$

This is related to the following variational formulation:

$$\int_\Omega (-\nabla.(D\nabla u(r)) + ku(r))\phi(r)d\Omega = \int_\Omega Bq(r)\phi(r)d\Omega. \tag{12}$$

By using Green's formula, we get:

$$\int_\Omega (D\nabla u(r).\nabla\phi(r) + ku(r)\phi(r))d\Omega - \int_{\partial\Omega} D\frac{\partial u}{\partial n}\phi(r)d\sigma = \int_\Omega Bq(r)\phi(r)d\Omega. \tag{13}$$

The Galerkin method consists in solving the variational problem defined by (13) by using the test-functions $\phi_i$, $i = 1, ..., N$.

This is equivalent to solving the linear system:

$$HU = L, \tag{14}$$

where $H$ denotes the $(N, N)$ matrix whose elements $H_{ij} = a(\phi_i, \phi_j)$, $L$ is the $N$ vector of coefficients $l(\phi_i)$, with

$a(u,v) = \int_\Omega (D\nabla u.\nabla v + kuv)d\Omega - \int_{\partial\Omega} D\frac{\partial u}{\partial n}vd\sigma$ and $l(v) = \int_\Omega Bq(r)vd\Omega$.

We can notice that the finite-element method is a variant of the Galerkin method in which the basis functions are some polynomial defined on a mesh.

Rather than using such an approach, we propose to define a function basis without any support of a mesh.

For that purpose, we consider a 1D eigenvalue problem defined by:

$$-\nabla.\nabla u(x) = \lambda u(x), \tag{15}$$
$$u(0) = u(1) = 0. \tag{16}$$

The eigenfunctions of this problem are:

$$u_i(x) = \sqrt{2}\sin(2i\pi x). \tag{17}$$

We can easily check that those eigenvalues define an orthonormal basis, since $\int_0^1 u_i(x)u_j(x)dx = \delta_{ij}$, where $\delta_{ij}$ is equal to 1 when $i = j$, otherwise 0.

By using the $u_i(x)$'s for solving the problem (12) where both $D$ and $k$ are constant over the domain $\Omega = [0,1]$, one get a linear system of the form (14), in which the matrix $H$ is diagonal with $H_{ii} = Di^2\pi^2 + k$.

This approach may be generalized in 2D (with $\Omega = [0,1]\times[0,1]$) or in 3D (with $\Omega = [0,1]\times[0,1]\times[0,1]$). In what follows, the direct model is denoted as:

$$HU = L. \tag{18}$$

## III. THE INVERSE PROBLEM

We have to solve the following infinite-dimensional least-square problem:

$$\min_{q,u\in L^2(\Omega)} \|y_m - y\|^2, \tag{19}$$
$$s.t.\ -\nabla.(D\nabla u(r)) + ku(r) = Bq(r),\ \forall r\in\Omega \tag{20}$$
$$u(r) = 0,\ \forall r\in\partial\Omega, \tag{21}$$
$$y = Cu(r),\ \forall r\in\partial\Omega. \tag{22}$$

### A. A Low Complexity Parametrization

Parametrization of the inverse problem is the key feature governing complexity. $q(r)$ is also chosen here as a combination of the same orthonormal basis functions:

$$q_a(r) = \sum_{i=1}^N q_i\phi_i(r). \tag{23}$$

It follows that $l(v) = \int_\Omega Bq(r)vd\Omega$, i.e.

$$l(v) = \sum_{i=1}^N q_i \int_\Omega B\phi_i(r)vd\Omega. \tag{24}$$

Finally $L(q)$ is approximated by $L_rQ$, where $Q = (q_1,...,q_N)^T$ and $L_r$ denotes the $(N,N)$ matrix with coefficients $L_{ij} = \int_\Omega B\phi_i(r)\phi_j(r)d\Omega$.

The $L_{ij}$'s can be easily computed when the $\phi_i(r)$'s are orthonormal functions: $L_{ij} = B\delta_{ij}$.

If $C = (\delta(r-r_1),...,\delta(r-r_m))^T$, the output equation $y = Cu$ is approximated as $y = C_rU$, where

$$C_r = \begin{pmatrix} \phi_1(r_1) & ... & \phi_N(r_1) \\ \vdots & ... & \vdots \\ \phi_1(r_m) & ... & \phi_N(r_m) \end{pmatrix}. \tag{25}$$

Finally the forward problem takes the following form:

$$HU = L_rQ, \tag{26}$$
$$y = C_rU. \tag{27}$$

### B. A Finite-Dimensional Formulation

From the two previous subsections, we get the following approximate inverse problem:

$$\min_{U,Q\in R^N} \|y_m - C_rU\|^2, s.t.\ HU - L_rQ = 0. \tag{28}$$

In practice, due to the ill-posedness of such problems, it is mandatory to introduce the largest possible number of measurements. For that purpose, several data-sets are collected. The inverse problem is thus formulated as follows:

$$\min_{U_l,Q\in R^N} \sum_{l=1}^M \|y_m^l - C_rU_l\|^2,$$
$$s.t.\ H_lU_l - L_rQ = 0,\ l = 1,...,M, \tag{29}$$

where $M$ denotes the number of data-sets, $H_l$ denotes the rigidity matrix corresponding to data-set $l$, and $y_m^l$ and $U_l$ are the measured output vector and the approximation solution corresponding to the $l$th data-set, respectively.

### C. Computation of the Inverse Problem

The inverse problem (29) may be equivalently expressed as:

$$\min_{Q\in R^N} \|\bar{y}_m - \bar{C}_r\bar{H}^{-1}\bar{L}_rQ\|^2. \quad (30)$$

where $\bar{H}$ is the block-diagonal matrix containing the $H_l$'s on the diagonal, $\bar{C}_r$ is a block-matrix of $M$ matrices $C_r$, $\bar{L}_r$ is a block-matrix of $M$ matrices $L_r$ and $\bar{y}_m$ denotes the vector of the $y_m^l$'s.

A standard computation technique consists in introducing a regularization of the problem:

$$\min_{Q\in R^N} \|\bar{y}_m - \bar{C}_r\bar{H}^{-1}\bar{L}_rQ\|^2 + \lambda\|Q\|^2, \quad (31)$$

where $\lambda > 0$ denotes the regularization coefficient.

The unique solution of the problem is then given by:

$$Q = (A^TA + \lambda I_d)^{-1}A^T\bar{y}_m, \quad (32)$$

with $A = \bar{C}_r\bar{H}^{-1}\bar{L}_r$.

Different techniques may be used to compute the solution of (29): the conjugated gradient method or other techniques adapted to large-scale problems such as the GMRES methods (Generalized Minimal RESidual, [8]).

## IV. AN EXAMPLE OF 2D BIOLUMINESCENCE TOMOGRAPHY

In order to demonstrate the effectiveness of the here-proposed approach, we consider the following bioluminescence tomography problem:

$$\min_{q\in L^2(\Omega)} \|y_m - y(x,y,q)\|^2, \quad (33)$$

where $u(r,q)$ is solution of

$$-\nabla.(D\nabla u(x,y)) + ku(x,y) = q(x,y),\ \forall x,y \in [0,10]^2 \quad (34)$$

$$u(x,y) = 0,\ \forall x,y \in \partial\Omega, \quad (35)$$

$$y = Cu(x,y). \quad (36)$$

The coefficients $D$ and $k$ are supposed to be known and constant. $m$ sensors are located on the domain periphery in order to form a square included in the domain $[0,10\ cm]^2$ with a distance of 1.5 cm with respect to the domain boundary.

An experiment is simulated where $M$ data-set are built by using a total of $M$ near infra-red wavelengths, ranging from 600-650 nm. Over the 600-650 nm range of wavelengths the absorption coefficient varied from 0.281 to 0.058 $cm^{-1}$ and the diffusion coefficient from 0.0199 to 0.0216 $cm^{-1}$ across the wavelengths used (see figure 4 for a FEM solution example corresponding to one of the data-sets).

The reconstruction problem consists in determining two distinct polyhedric sources $P_1$ and $P_2$ on the domain $R_1 = [0,10\ cm]^2$, according to figure 2.

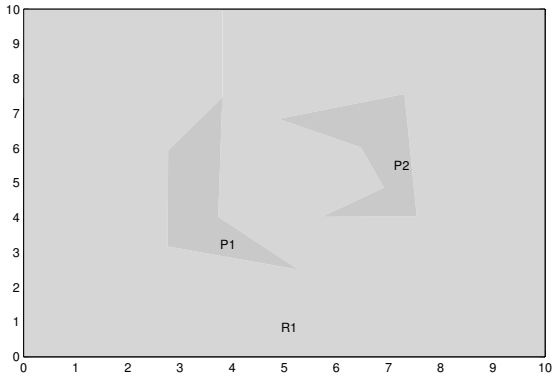


Fig. 2. Sources to be reconstructed

The measurement vector $\bar{y}_m$ is obtained in simulation from $M$ reference solutions defined by $M$ couples $(D_l, k_l)$, $l = 1,...M$, provided by the FEM (with pdetool under MATLAB) and the mesh corresponding to figure 3.

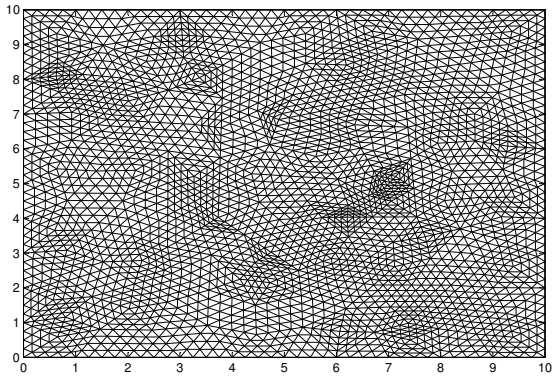

Fig. 3. FEM mesh of the problem

### A. The Forward Model

The Galerkin method is used with the orthonormal function basis inspired by the eigenfunctions of the operator $-\nabla.\nabla$ with Dirichlet boundary conditions:

$$\phi_{i,j}(x,y) = \sin(i\frac{\pi x}{10}) \times \sin(j\frac{\pi y}{10})/5,\ i,j = 1,...N. \quad (37)$$

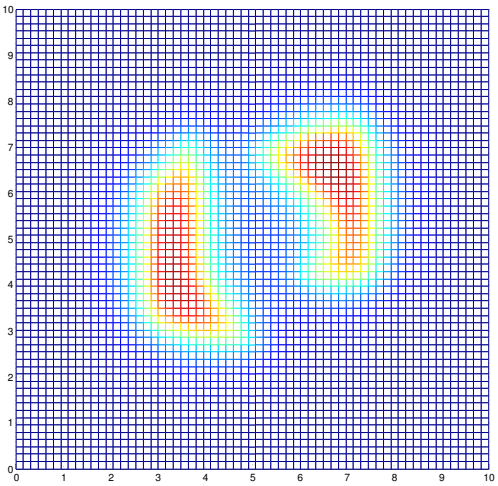

Fig. 4. A FEM solution example

We can easily check that:

$$\int_0^1 \int_0^1 [\sin(i\frac{\pi x}{10}) \times \sin(j\frac{\pi y}{10})/5] \times [\sin(k\frac{\pi x}{10}) \times \sin(l\frac{\pi y}{10})/5)]dxdy = \delta_{ij,kl}, \quad (38)$$

where $\delta_{ij,kl}$ is equal to 1 when both $i = k$ and $j = l$, otherwise 0.

The approximate solution $u_a(x, y)$ is defined as a linear combination of the form:

$$u_a(x, y) = \sum_{i=1}^{N} \sum_{j=1}^{N} u_{ij}\phi_{ij}(x, y). \quad (39)$$

It follows that the matrix $H$ is diagonal with coefficients:

$$H_{kk} = D(i^2 + j^2)\pi^2/100 + k. \quad (40)$$

First of all, we will consider quality of the solution according to the number of basis functions, compared to a FEM reference solution of the test problem described by figure 5.

Figures 6, 7 and 8 show that for $N = 20$ the Galerkin method provides results closed to the reference solution. Apart from $N = 20$, increasing $N$ does not bring very significant improvement of the solution.

We can emphasize the fact that:

1) the number of states required for a solution quality similar to the one of the FEM is reduced with a factor $7,24$, when taking $N = 20$.
2) the rigidity matrix $H$ is diagonal, when the coefficients $D$ and $k$ are constant over the domain.
3) A grid is not needed.

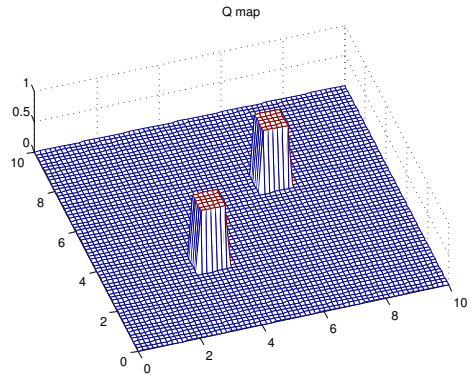


Fig. 5. Sources of the test problem

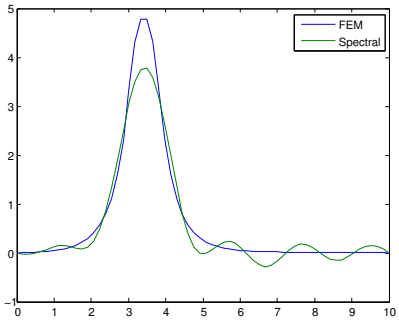


Fig. 6. $N = 10$, at coordinate $y = 3, 5$

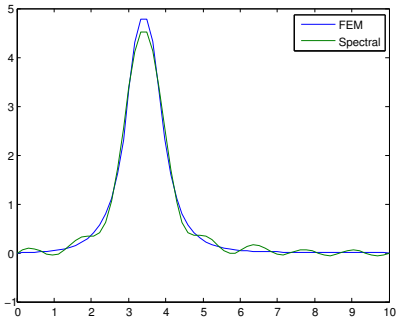


Fig. 7. $N = 15$, at coordinate $y = 3, 5$

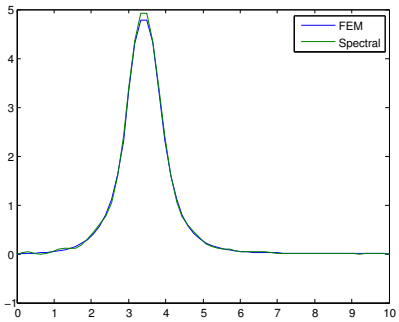


Fig. 8. $N = 20$, at coordinate $y = 3, 5$

### *B. Solution of the Inverse Problem*

The sources are reconstructed by using the approximate solution $q_a(r) = \sum_{i=1}^{N} q_i \phi_i(r)$, leading to a very simple matrix $L_r = I_d$.

Figures 9 and 10 present reconstruction results obtained with two values of the number of basis functions $N$. $M = 49$ data-sets have been generated.

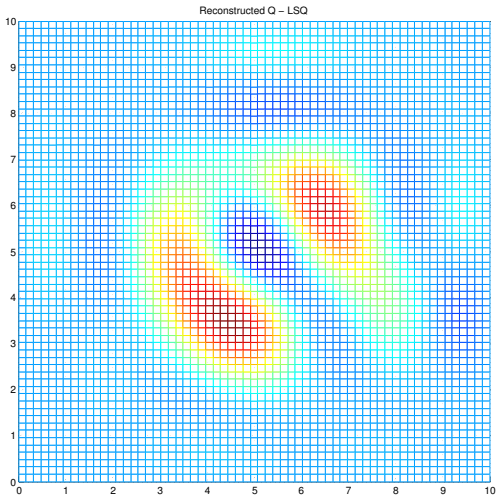


Fig. 9. Reconstruction with $N = 7$ and $M = 49$ data-sets

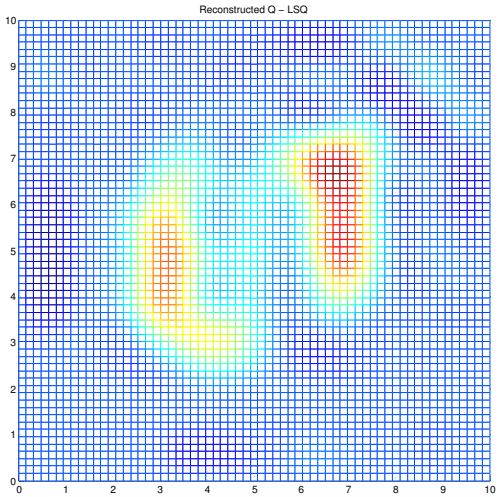


Fig. 10. Reconstruction with $N = 12$ and $M = 49$ data-sets

A clear improvement of the reconstruction is obtained by increasing the number of basis functions. Increasing either $N$ or $M$ do not provide significant improvements to the reconstruction process. The overall computation time is less than one minute under MATLAB using an Intel Pentium 1600 Mhz, 512 Mo RAM, for the worst case $N = 12$ and $M = 49$.

## V. CONCLUSIONS

A tomography method with low complexity has been proposed in this paper. This method is not based on a complex grid as it is the case for the finite-element method. Thanks to the use of an orthonormal basis, a very simple forward model has been defined, allowing simple computation of the associated inverse problem. A 2D bioluminescence tomography problem demonstrates very encouraging results with reduced computation time compared to classical approaches based on the finite-element method. Generalization of the approach for 3D inverse problems is straightforward.

## REFERENCES

[1] S. R. Arridge, Optical tomography in medical imaging, *Inverse Problems*, vol. 15, pp. 41–93, April 1999.
[2] H. Grandin, *Fundamentals of the Finite Element Method,* Macmillan, New York, 1986.
[3] Ge Wang, Wenxiang Cong, Yi Li, Weimin Han, Durai Kumar, Xin Qian, Haiou Shen, "Recent development in bioluminescence tomography", *3rd IEEE International Symposium on Biomedical Imaging: Nano to Macro*, pp. 678–681, 2006.
[4] W. Wehlau, and J. Rice, Zeeman Doppler Imaging, *Peculiar versus Normal Phenomena in A-type and Related Stars*, vol. 44, pp. 247–257, 1993.
[5] T. F. Coleman, and Y. Li, An Interior, Trust Region Approach for Nonlinear Minimization Subject to Bounds, *SIAM Journal on Optimization*, vol. 6, pp. 418–445, 1996.
[6] A. Frassati, A. Da Silva, J.-M. Dinten, D. Georges, "Wavelet-based Model Reduction Applied to Fluorescence Diffuse Optical Tomography", *Proceedings of the European Control Conference 2007*, Kos, Greece, July 2-5, 2007.
[7] A. Frassati, A. Da Silva, J.-M. Dinten, D. Georges, "Model Reduction by Multiresolution Method Applied to Fluorescence Diffuse Optical Tomography", *IEEE Engineering in Medicine and Biology Conference*, Lyon, France, 2007.
[8] Y. Saad, M.H. Schultz, GMRES: A Generalized Minimal Residual algorithm for solving nonsymmetric linear systems, *SIAM J.Sci.Stat.Comput.*, vol. 7, no. 3, pp. 856–869, July 1986.
[9] R.B. Schulz, J. Ripoll, and V. Ntziachristos, Experimental fluorescence tomography of tissues with noncontact measurements, *IEEE Transactions On Medical Imaging*, vol. 23, no. 4, pp. 492–500, Apr. 2004.
[10] M. J. Eppstein, F. Fedele, J. Laible, C. Zhang, A. Godavarty, and E. M. Sevick-Muraca, A Comparison of Exact and Approximate Adjoint Sensitivities in Fluorescence Tomography, *IEEE Transactions On Medical Imaging*, vol. 22, no. 10, pp. 1215–1223, Oct. 2003.
[11] C.A.J. Fletcher, *Computational Galerkin Methods,* Springer Verlag, N. Y./Berlin/Heidelberg, 1984.
[12] D. Patella, Introduction to ground surface self-potential tomography, *Geophysical Prospecting*, vol. 45, pp. 653–681, 1977.
[13] A. N. Tikhonov, V. Y. Arsenin, *Solution of Ill-Posed Problems,* Wiley, New York, 1977.
[14] Y. Wang, J. Chang, R. Aronson, R. L. Barbour, H. L. Graber, and J. Lubowsky, "Imaging scattering media by diffusion tomography: An iterative perturbation approach", *Proc. of SPIE Conf; Physiological Monitoring and Early Detection Diagnostic Methods*, vol. SPIE-1641, pp. 58–71, jan. 1992.
[15] W. Zhu, Y. Wang, H. L. Graber, R. L. Barbour, and J. Chang, "A regularized progressive expansion algorithm for recovery of scattering media form time-resolved data", *Proc. of OSA Topical Meeting on Advances in Optical Imaging and Photon Migration*, pp. 211–216, Mar. 1994.